Spontaneous Ordering of Oxide Nanostructures

S. Aggarwal,[1]* A. P. Monga,[1] S. R. Perusse,[1] R. Ramesh,[1] V. Ballarotto,[2] E. D. Williams,[2] B. R. Chalamala,[3] Y. Wei,[3] R. H. Reuss[3]

We report the spontaneous formation of uniformly distributed arrays of "tips" (tall conical hillocks) upon oxidation of palladium (Pd) thin films. The formation of the palladium oxide tips depended on the thickness and granularity of the Pd film and on annealing and oxidation conditions. As the Pd film thickness increased from 40 to 200 nanometers, the average height of the tips increased from 0.5 to 1.2 micrometers, their height distribution became broader, and their density decreased from 55×10^6 to 12×10^6 per square centimeter. Enhanced photoelectron emission from locations corresponding to the tips suggests their possible use in field emission applications.

In contrast to artificially ordered schemes, such as those currently used in integrated circuits, "self-assembled" processes may enable the creation of complex device architectures that rely on the intrinsic ability of the system to organize itself into ordered patterns. Many inorganic systems display microstructural evolution that resembles "self-assembled" processes—for example, dendrite formation in melts, spinodal decomposition in alloys, and martensitic twins in metallic and ceramic alloys, where the "assembly" process is driven by thermodynamic and kinetic considerations.

We report the "self-assembly" of micrometer-scale hillocks of conducting palladium oxide (PdO_2). Formation of hillocks in metal films is generally attributed to the relaxation of thermal expansion mismatch stresses between the substrate and the film (*1*). The compressive stresses that develop during heating lead to diffusion of metal atoms either through the lattice (*2, 3*) or along grain boundaries (*4*), leading to the formation of hillocks. Typically these are discrete, isolated hillocks of the metal. We report the results of experiments aimed at exploiting hillock formation to create arrays of high–aspect ratio hillocks (or tips) of materials that may enable self-assembled nanotechnologies. We found that hillocks can be formed via the oxidation of thin films of metals such as Pd, Ir, In, and Fe that can form oxides with anisotropic crystal structures. The anisotropy of the oxide promotes oxygen diffusion along certain crystallographic planes as opposed to others. The large volume change accompanying oxidation of these metals leads to large compressive stresses that are relaxed by the formation of hillocks, which are as high as ~2 μm in some cases. Here, Pd metal films (40 to 200 nm) were deposited by pulsed laser ablation at room temperature in vacuum (10^{-6} torr) on oxide substrates such as MgO and $LaAlO_3$ and subsequently annealed in oxygen at temperatures between 600° and 900°C. The films were characterized using x-ray diffraction (XRD), atomic force microscopy (AFM), and photoelectron emission microscopy (PEEM).

An AFM image of a polycrystalline Pd film (120 nm) deposited on a $LaAlO_3$ substrate after it had been annealed in O_2 at 900°C for 1 hour (Fig. 1) reveals that oxidation is accompanied by the formation of a uniform array of surface features (tips) that resemble the Si (*5, 6*) and Mo (*7*) cones in a field emitter array and, on a different scale, InAs islands on GaAs (*8*). The tips are ~1 μm high and are uniformly spaced, with a periodicity of ~2 μm. XRD studies of these films indicate that the entire Pd film is oxidized and that the tips are polycrystalline palladium oxide structures, so we assume that the tips are isolated and the surface seen in the AFM image is that of $LaAlO_3$. They are distinctly different from the hillocks reported earlier in their periodicity, height, and composition. The hillocks reported in metal thin films are generally discrete and isolated (for example, a single tip over several millimeters) and their height is always less than ~100 nm (*1*).

To quantify the parameters governing hillock formation, we carried out several simple experiments on Pd thin films. The first set of experiments was aimed at understanding the effect of film granularity on the formation of these tips. Pd films (800 Å) were grown on single-crystal {100} MgO surfaces at room temperature to obtain a polycrystalline microstructure, and also at 725°C to obtain epitaxial [001] growth (which was confirmed by ϕ angle x-ray scans). The films were then annealed either in oxygen or in vacuum at 900°C for 1 hour to create the surface morphologies. Vacuum annealing formed hillocks less than 100 nm high on the surface of the epitaxial film (Fig. 2A); these were confirmed by XRD to be Pd metal. The epitaxial film annealed in oxygen (Fig. 2B) was very different from the film imaged in Fig. 1; there was very little indication of the formation of hillocks, and apparently only the roughness of the film increased. Polycrystalline Pd films behaved differently: Vacuum annealing formed hillocks ~150 nm high

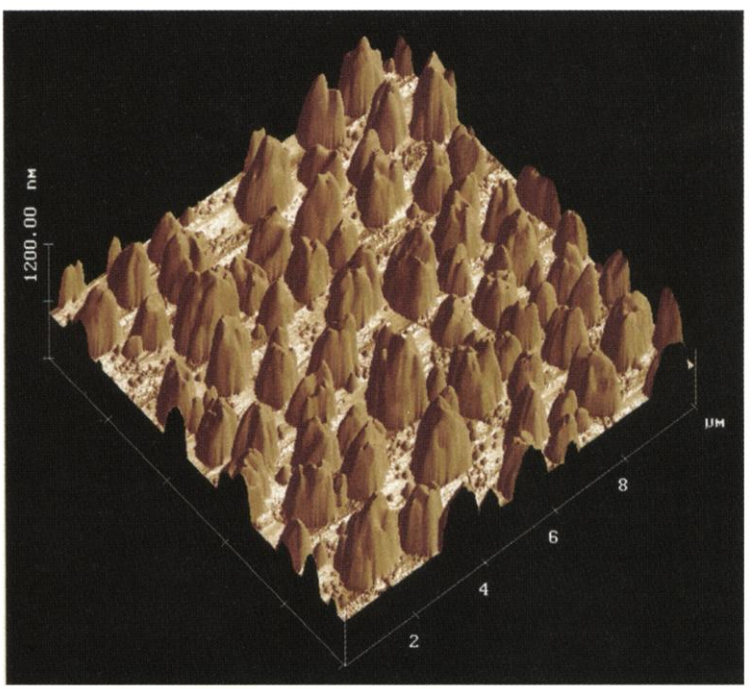

Fig. 1. AFM image of a Pd film annealed in oxygen at 900°C, showing uniformly spaced tips ~1 μm high.

[1]Department of Materials and Nuclear Engineering, [2]Department of Physics, University of Maryland, College Park, MD 20742, USA. [3]Flat Panel Display Division, Motorola Inc., 7700 South River Parkway, Tempe, AZ 85284, USA.

*To whom correspondence should be addressed. E-mail: aggarwal@eng.umd.edu

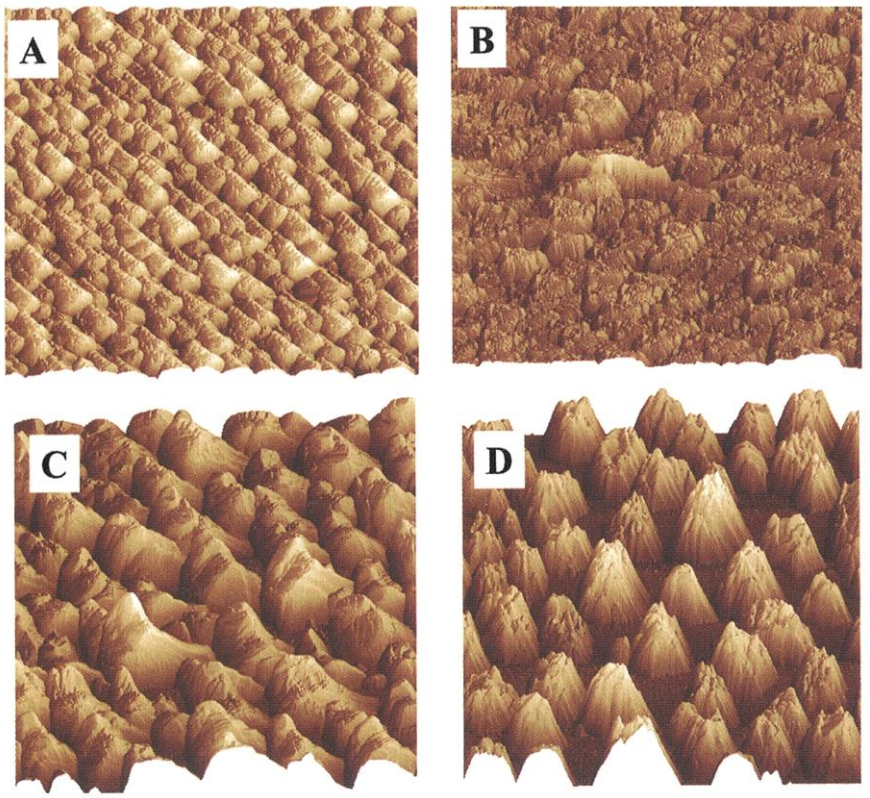

Fig. 2. AFM images (10 μm by 10 μm; z range, 0.7 μm) of Pd films of varying crystallinity and annealing ambient at 900°C for 1 hour: (**A**) epitaxial film annealed in vacuum, (**B**) epitaxial film annealed in oxygen, (**C**) polycrystalline film annealed in vacuum, and (**D**) polycrystalline film annealed in oxygen.

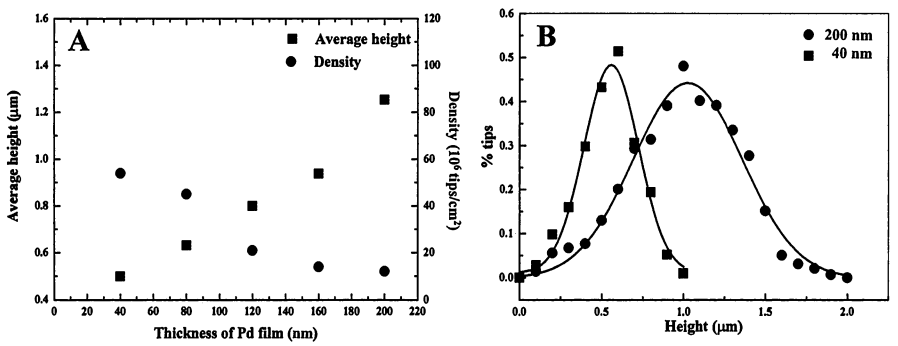

Fig. 3. (**A**) Average height and density of the tips plotted as a function of Pd film thickness. (**B**) The height distribution for the thickest and thinnest film.

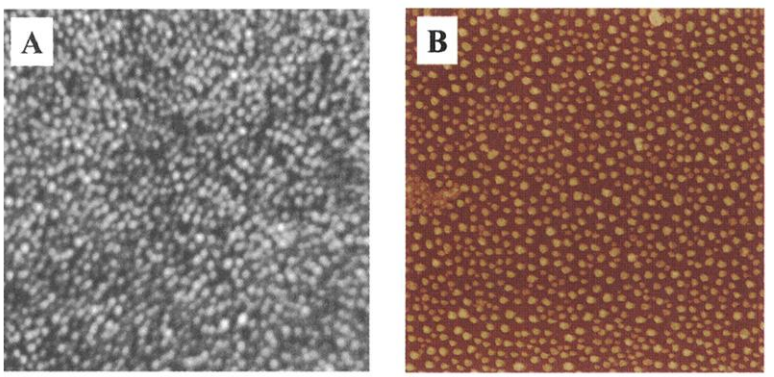

Fig. 4. (**A**) PEEM image and (**B**) AFM image (50 μm by 50 μm) of a Pd film (80 nm) annealed in oxygen at 900°C for 1 hour.

(Fig. 2C), whereas oxygen annealing yielded hillocks 1 μm high (Fig. 2D). Because tips were formed only when the starting Pd film was polycrystalline, the transport of Pd atoms or ions may be more rapid by grain boundary diffusion.

Studies of the spontaneous ordering of semiconductor nanostructures have established that long-range elastic interaction is the driving force for ordering (*9*). However, the details of the ordering of such arrays are the subject of much debate (involving thermodynamic and kinetic considerations) and therefore are not discussed here. Nevertheless, the above experiments demonstrate one important difference between the tips formed in this study and the hillocks formed in metal and semiconductor films. In metals, the hillocks are reported to form as the result of relaxation of compressive stresses due to thermal expansion mismatch between the substrate and the film (*1*). In our case, hillocks formed with similar heights and spacing on both $LaAlO_3$ and MgO substrates, which have thermal expansion coefficients of 10×10^{-6} per °C (*10*) and 13.8×10^{-6} per °C (*11*), respectively. Pd has a thermal expansion coefficient of $\sim 11.76 \times 10^{-6}$ per °C (*12*), which leads to a compressive stress in the case of $LaAlO_3$ but a tensile stress in the case of MgO. This difference implies that both the source and the magnitude of the driving force for forming hillocks are very different in our case. The oxidation of Pd to PdO_2 is accompanied by a 38% volume change; this is the primary reason for the formation of tips, because the compressive stresses introduced by the volume change are larger than those arising from thermal expansion mismatch.

To understand the factors that control the size (base diameter) and height distribution, we studied the evolution of these parameters with thin-film processing conditions including controls on film thickness, annealing temperature, and ambients. A plot of film thickness versus the average height of the tips (Fig. 3A) shows a progressive increase in height, with an average height of ~1.2 μm for the thickest film. After oxidation, the height distribution of the tips for the 200-nm and 40-nm Pd films (Fig. 3B) shows that although the average height of the tips becomes greater with increasing film thickness, the shape of the distribution curve for the tip height becomes broader. This result suggests that thinner films would lead to a narrow distribution of tips and implies that high–aspect ratio tips of PdO_2 can be self-assembled with this process. Also plotted in Fig. 3A is the density (number of tips of average height and above), which decreases from $\sim 55 \times 10^6$ to $\sim 12 \times 10^6$ tips/cm^2. With increasing film thickness, we observed that the size (base diameter) distribution becomes narrower. These observations are consistent with an Ostwald ripening process (*13*), which suggests that the tips are approaching a specific mean size.

One potential application of these arrays is as field emitter arrays for vacuum microelectronic devices. The possibility that large arrays can be self-assembled using simple thin-film processes without the need for expensive lithography makes them interesting for the field emission display industry (*14*). Currently, metal field emitters are fabricated using an elaborate process [the Spindt process (*7*)] involving photolithographic definition of individual emitter wells and the subsequent deposition of the refractory metals to form the periodic arrays of emitters. An intrinsic feature of the Spindt process is the need to carry out expensive micrometer- or submicrometer-scale photolithography, which is not cost-effective for large-area displays. To explore the feasibility of field-assisted electron emission, we obtained PEEM images from these arrays under an applied field of 30 kV/cm and ultraviolet light of energy ~5 eV. Because the surface work function of PdO_2 is ~3.9 eV (*15*), the tips were expected to emit electrons under these conditions. The PEEM image (Fig. 4A) shows a distribution of bright spots with a typical spacing of about 1.5 to 2.5 μm, which is consistent with the spacing of the tips as measured from AFM images (Fig. 4B). The less bright spots are perhaps emission from the edges of the tips. Analysis of bright-field patterns in the PEEM images reveals the bright-field spot density to be $\sim 47 \times 10^6$ tips/cm^2. This result is consistent with the density of tips determined from the AFM images for the same sample, which we estimate (number of tips of average height and above) to be $\sim 46 \times 10^6$ tips/cm^2. This density of tips or field emitter cones is well within the specifications for current field emission displays, which require $\sim 6 \times 10^6$ tips/cm^2 (based on current density of 1 μA) for each subpixel (50 μm by 300 μm) for a 15-inch SVGA monitor (*14*). To further justify the use of these tips as field emission arrays, we have controlled the tip-to-tip distance, their aspect ratio, and the tip radius by controlling the thickness and grain size of the starting Pd film. Finally, these emitters can be gated using a scheme similar to that used for Si field emitter arrays (*5*).

References and Notes

1. F. M. d'Heurle, *Int. Mater. Rev.* **34**, 53 (1989) and references therein.
2. F. R. N. Nabarro, in *Report of a Conference on Strength of Solids* (The Physical Society, London, 1948), p. 75.
3. C. Herring, *J. Appl. Phys.* **21**, 437 (1950).
4. R. L. Coble, *J. Appl. Phys.* **34**, 1679 (1963).
5. D. Temple, *Mat. Sci. Eng.* **R24**, 185 (1999).
6. M. R. Rakhshandehroo, J. W. Weigold, W.-C. Tian, S. W. Pang, *J. Vac. Sci. Technol. B* **16**, 2849 (1998).
7. C. A. Spindt, *J. Appl. Phys.* **39**, 3504 (1968).
8. Q. Xie, A. Madhukar, P. Chen, N. P. Kobayashi, *Phys. Rev. Lett.* **75**, 2542 (1995).
9. V. A. Schhukin and D. Bimberg, *Rev. Mod. Phys.* **71**, 4 (1999), and references therein.
10. B. C. Chakoumakos, D. G. Schlom, M. Urbanik, J. Luine, *J. Appl. Phys.* **83**, 1979 (1998).
11. K.-H. Hellwege and A. M. Hellwege, Eds., *Landolt-Bornstein Numerical Data and Functional Relationships in Science and Technology* (Springer-Verlag, New York, 1975), vol. 7, p. 26.
12. L. Holborn and A. L. Day, *Ann. Phys.* **4**, 104 (1901).
13. I. M. Lifschitz and V. V. Slyozov, *Phys. Chem. Solids* **19**, 35 (1961).
14. B. R. Chalamala, Y. Wei, B. E. Gnade, *IEEE Spectrum* **35**, 42 (1998).
15. J. H. Bernhard, E. D. Sosa, D. E. Golden, B. R. Chalamala, Y. Wei, R. H. Reuss, S. Aggarwal, R. Ramesh, unpublished data.

16. Supported in part by NSF Materials Research Science and Engineering Center grant DMR96-32521 and Laboratory for Physical Sciences and by a University of Maryland Distinguished Research Faculty Fellowship (R.R.).

15 November 1999; accepted 4 February 2000

Generation of Femtosecond Pulses of Synchrotron Radiation

R. W. Schoenlein,[1]* S. Chattopadhyay,[2] H. H. W. Chong,[4] T. E. Glover,[3] P. A. Heimann,[3] C. V. Shank,[1] A. A. Zholents,[2] M. S. Zolotorev[2]

Femtosecond synchrotron pulses were generated directly from an electron storage ring. An ultrashort laser pulse was used to modulate the energy of electrons within a 100-femtosecond slice of the stored 30-picosecond electron bunch. The energy-modulated electrons were spatially separated from the long bunch and used to generate ~300-femtosecond synchrotron pulses at a bend-magnet beamline, with a spectral range from infrared to x-ray wavelengths. The same technique can be used to generate ~100-femtosecond x-ray pulses of substantially higher flux and brightness with an undulator. Such synchrotron-based femtosecond x-ray sources offer the possibility of applying x-ray techniques on an ultrafast time scale to investigate structural dynamics in condensed matter.

An important scientific frontier is the application of x-ray pulses to investigate ultrafast structural dynamics (atomic motion and rearrangement) associated with phase transitions in solids, chemical reactions, and rapid biological processes. The fundamental time scale for such motion is an atomic vibrational period, on the order of 100 fs. Such dynamics have been investigated to date primarily with visible pulses from mode-locked femtosecond lasers (*1*) that probe only extended electronic states providing indirect information about atomic structure. X-rays, on the other hand, interact with core electronic levels and can therefore provide direct information about atomic structure. Rapid advances in our understanding of condensed matter structure at the atomic scale have been driven by modern synchrotrons providing high-brightness x-ray beams (*2*). However, the time resolution available from synchrotrons is nearly three orders of magnitude too slow to probe atomic motion within a single vibrational period. Recent efforts at applying x-rays to probe structural dynamics have used a synchrotron source combined with a picosecond-resolution x-ray streak camera (*3*) or relatively low brightness subpicosecond x-ray sources based on laser-produced plasmas (*4, 5*), laser-driven diodes (*6*), and relativistic Thomson scattering (*7, 8*). We demonstrate the generation of femtosecond pulses at a synchrotron beamline using femtosecond laser pulses (*9*), which is a promising approach to extend the time resolution of high-brightness synchrotron x-ray sources to 100 fs and will enable the study of structural dynamics through time-resolved x-ray diffraction, extended x-ray absorption fine structure (EXAFS), and related x-ray spectroscopies using pump-probe techniques.

The duration of x-ray pulses generated by synchrotrons is determined by the duration of each stored electron bunch, typically >30 ps. Storage of ultrashort bunches of appreciable charge in a ring is problematic because of instabilities arising from bunch-induced wake fields (*10*). However, short electron bunches can exist in a storage ring for a limited time. We demonstrate experimentally that a femtosecond laser pulse can be used to create femtosecond time structure on a long electron bunch through energy modulation of an ultrashort slice of the bunch. Femtosecond synchrotron pulses (with a spectral range extending from infrared to x-ray wavelengths) are then generated from the ultrashort electron slice. As the modulation rapidly dissipates because of the dynamics of electrons within the storage ring, the electron bunch completely recovers between laser interactions. Furthermore, because the modulation is created by a femtosecond optical pulse, there is absolute synchronization between the x-ray probe pulses

[1]Materials Sciences Division, [2]Accelerator and Fusion Research Division, [3]Advanced Light Source, Ernest Orlando Lawrence Berkeley National Laboratory, Berkeley, CA 94720, USA. [4]Applied Science and Technology Graduate Group, University of California Berkeley, Berkeley, CA 94720, USA.

*To whom correspondence should be addressed. E-mail: rwschoenlein@lbl.gov